

Received July 16, 2020, accepted July 30, 2020, date of publication August 11, 2020, date of current version August 21, 2020.

Digital Object Identifier 10.1109/ACCESS.2020.3015754

Two-Dimensional Joint Acquisition of Doppler Factor and Delay for MC-DS-CDMA in LEO Satellite System

ENTONG MENG^{ID} AND XIANGYUAN BU^{ID}, (Member, IEEE)

School of Information and Electronics, Beijing Institute of Technology, Beijing 100081, China

Corresponding author: Xiangyuan Bu (bxy@bit.edu.cn)

This work was supported by the National Natural Science Foundation of China under Contract U1836201.

ABSTRACT Low Earth Orbit (LEO) satellite systems have received considerable attentions for its advantages and potential applications in global communication. Yet LEO satellite-ground communication is challenged by the huge Doppler shift. This article is devoted to studying how to deal with this challenge in Multi-carrier Direct Sequence Code Division Multiple Access (MC-DS-CDMA) systems in the presence of multi-path and partial band interferences for LEO satellite-ground link in urban areas. To this end, we design a two-dimensional joint acquisition algorithm. Specifically, we acquire the delay and Doppler factor by solving the Maximum Likelihood (ML) problem with decision variable falling into two-dimensional uncertain region of the estimated parameters. We then use grid-based searching method to access the ML estimates of the delay and Doppler factor at the cost of acceptable complexity. We also derive the detection probability and Mean Square Error (MSE) in both Additive White Gaussian Noise (AWGN) and Rayleigh fading channels. It is shown that the performance of MC-DS-CDMA with the proposed algorithm significantly outperforms its single-carrier counterpart in Rayleigh fading channel, and is proved to be more tolerant to partial band interferences for both AWGN and Rayleigh fading scenarios.

INDEX TERMS Low Earth orbit (LEO) satellite system, multi-carrier direct sequence code division multiple access (MC-DS-CDMA), two-dimensional joint acquisition, detection probability, mean square error (MSE).

I. INTRODUCTION

Low Earth Orbit (LEO) satellites play an important role in providing global communication services [1]. In recent years, more than 20 enterprises have submitted applications to Federal Communications Commission (FCC) for the permission of accessing Non-geostationary Orbit (NGSO) market, including Boeing, O3b, SpaceX [2], [3] and OneWeb [4]. For the existing LEO satellite communication systems, Single-carrier Direct Sequence Code Division Multiple Access (SC-DS-CDMA) technique has been widely employed for its advantages of providing higher capacity and easier network planning over its conventional counterparts like Single-carrier Time Division Multiple Access (SC-TDMA) and Single-carrier Frequency Division Multiple Access (SC-FDMA). However, the complex channel characteristics of LEO satellite link in urban areas challenge the SC-DS-CDMA systems. Specifically, in urban areas,

the direct line between the ground terminal and the LEO satellite is almost completely obstructed by high buildings and multistory residences. Therefore, electromagnetic energy propagation in urban areas is largely by way of scattering [5], [6], and the multi-path channel between satellite and ground terminal would be frequency-selective whenever the bandwidth of signal exceeds the coherent bandwidth of the channel. Besides, the inherent anti-interference capability deriving from correlating received signal with predefined spreading sequence is also quite limited. This means the adverse effect introduced by Partial Band Interference (PBI) would fail to be completely eliminated, especially in the presence of strong interferences. To overcome these drawbacks, Multi-carrier Direct Sequence Code Division Multiple Access (MC-DS-CDMA) system has been proposed [7]–[11], where the acquisition (coarse synchronization) of MC-DS-CDMA is essential to the correct recovery of received signal. Meanwhile, the acquisition is rather difficult due to the presence of Doppler shift incurred by high relative movement between LEO satellite and ground

The associate editor coordinating the review of this manuscript and approving it for publication was Nan Wu^{ID}.

devices [12]. Several works have studied the synchronization problems for MC-DS-CDMA [13], [14]. Nevertheless, these analyses assume that the acquisition of received MC-DS-CDMA signal has already been completed. Works [15]–[17] have designed the joint code acquisition algorithms based on non-coherent sub-carrier combining for MC-DS-CDMA. However, they do not consider the impact of Doppler shift, and cannot be used in LEO satellite-ground communication systems.

Against these deficiencies, in this article we propose a two-dimensional joint acquisition algorithm for MC-DS-CDMA system to obtain the coarse estimates of Doppler factor and delay, which is applicable for LEO satellite-ground communication systems. The contributions of this article are listed below:

1) Two-dimensional joint acquisition algorithm for MC-DS-CDMA system is proposed in this article, in which the coarse estimates of Doppler factor and delay could be obtained concurrently by solving the Maximum Likelihood (ML) problem deriving from observations collected from all sub-carriers.

2) The solution of ML problem claims for a continuous two-dimensional brute search. And the computing complexity of this exhaustive search seems to be formidable. To counteract this defect, a practical two-dimensional grid-based searching scheme is further provided for the sub-optimal ML estimates of Doppler factor and delay.

3) The detection probability and Mean Square Error (MSE) performance of the proposed algorithm are analyzed in comparison with that of SC-DS-CDMA system in urban LEO satellite system in presence of multi-path fading, Doppler shift and PBI. It is shown that the MC-DS-CDMA with the proposed algorithm has superior performance to SC-DS-CDMA system in multi-path fading case, and is proved to be more resistant to PBI for both Additive White Gaussian Noise (AWGN) and multi-path scenarios.

The rest of this article is organized as follows. In Section II, the system model of discussed MC-DS-CDMA is profiled. Given the potent formation in system model, in Section III, we propose a two-dimensional joint acquisition algorithm for MC-DS-CDMA and detail an achievable scheme with an acceptable computing complexity. The performance of the proposed algorithm is investigated in Section IV, involving the detection probability and MSE values of Doppler factor as well as delay in both AWGN and multi-path fading channels. Finally, the corresponding numerical results are provided in Section V, and performance comparison with single-carrier system is also conducted in this discourse.

II. SYSTEM MODEL

A. TRANSMITTER

The MC-DS-CDMA system considered here transmits DS signal of k th user on U sub-carriers. It is assumed that the U associated sub-bands are disjoint in frequency and the signal in each sub-band is bandlimited. Therefore, there exists no

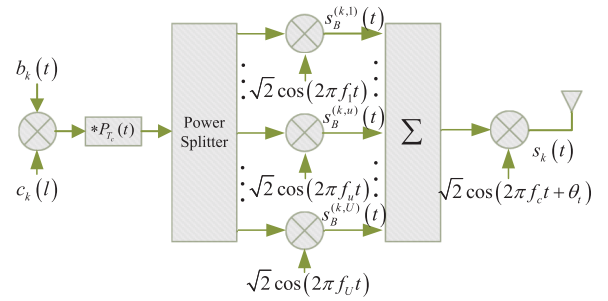


FIGURE 1. Diagram of MC-DS-CDMA transmitter for k th user.

self-interference affecting the signals in other sub-bands [15]. The diagram of MC-DS-CDMA transmitter for k th user is demonstrated in Figure 1, and the transmitted signal $s_k(t)$ is given by

$$s_k(t) = \sum_{u=1}^U \sqrt{2} s_B^{(k,u)}(t) \cos(2\pi f_c t + \theta_t) \quad (1)$$

where f_c denotes the Radio Frequency (RF) of MC-DS-CDMA transmitted signal, while θ_t is a random phase caused by up-conversion and is uniformly distributed over $[0, 2\pi)$; $s_B^{(k,u)}(t) = \sqrt{\frac{2P}{U}} b_k(t) c_k(t) \cos(2\pi f_u t)$ denotes the baseband transmitted sub-carrier signal for k th user, where $\sqrt{\frac{P}{U}}$ is the associated sub-carrier transmitted power; $b_k(t)$ is the data waveform consisting of a sequence of mutually independent rectangular pulses of duration T_s , $f_u = \{f_1, f_2, \dots, f_U\}$ denotes the baseband center frequencies of associated sub-carriers; $c_k(t) = \sum_{l=0}^{L-1} c_k(l) P_{T_c}(t - lT_c)$ is the signature waveform employed by sub-carriers of k th user, where L is the spreading gain, $T_c = \frac{T_s}{L}$ is the chip period, and $c_k(l) \in \{-1, 1\}$. Here we use $P_{T_c}(t)$ to denote the impulse response of the bandlimited Chip Pulse Shaping Filter (CPSF), which is typically a unit-energy Square Root Raised Cosine (SRRC) waveform having a roll-factor of λ and time-supported over the interval of $[0, DT_c]$ with $D \in \{1, 2, 3, \dots\}$ and $2D \leq L$ [18].

B. CHANNEL

The channel model discussed is the LEO satellite link in urban areas exhibiting Doppler shift, multi-path fading and Gaussian PBI. Given the direct line between the ground terminal and the satellite is almost completely obstructed by high buildings and multistory residences, the receiver could only pick up reflected signals from all directions in the horizontal plane. Therefore, the envelope of the received signal undergoes fading with a Rayleigh statistical distribution [5], [6]. And the channel is deemed as a slowly varying frequency-selective Rayleigh channel in which the signal in each sub-band is non-frequency-selectively fading and independently. Therefore, the Channel Impulse Response (CIR) matched to user k and sub-carrier u is defined as

$$h_{k,u}(t) = \alpha_{k,u} \delta[(1 + \beta)t] \exp(-j\varphi_{k,u}) \quad (2)$$

where $\beta = \frac{v}{c}$ (v is the relative speed between transceiver while c is the speed of light) is the Doppler factor; $\alpha_{k,u}$ denote Independently Identically Distributed (IID) Rayleigh random variables with a unit second moment while $\varphi_{k,u}$ is the IID uniform random variables over $[0, 2\pi)$. Notedly, $\alpha_{k,u}$ and $\varphi_{k,u}$ would be ignored in terms of non-multi-path fading AWGN channel. We consider the first user is the user of interest. Therefore, the baseband form of the received signal could be provided as (3) under the hypothesis that the code-frequency offset caused by Doppler shift is so small that it can be negligible [19], and there is no data modulation adopted during acquisition process (i.e., $b_1(t) = 1$).

$$r(t) = \sum_{u=1}^U \alpha_{1,u} \sqrt{\frac{P}{U}} c_1(t - \tau_1) \exp[j2\pi\beta(f_u + f_c)t + j\theta_{1,u}] + I(t) + w(t) + J(t)$$

$$I(t) = \sum_{k=2}^K \sum_{u=1}^U \alpha_{k,u} \sqrt{\frac{P}{U}} b_k(t - \tau_k) c_k(t - \tau_k) \times \exp[j2\pi\beta(f_u + f_c)t + j\theta_{k,u}] \quad (3)$$

where τ_k denotes the unknown delay for user k uniformly distributed over $[0, T_s)$; $\theta_{k,u} = -2\pi\beta f_c \tau_k - 2\pi f_u(1 + \beta)\tau_k + \theta_t - \theta_r - \varphi_{k,u}$ is the random phase which is uniformly distributed over $[0, 2\pi)$ while θ_r is derived from the process of down-conversion; $w(t)$ represents AWGN with zero mean and a double-sided power spectral density of $\frac{\eta_w}{2}$; $J(t)$ denotes Gaussian PBI having power spectral density of

$$S_J(f) = \begin{cases} \frac{\eta_J}{2}, & f_J - \frac{W_J}{2} \leq f \leq f_J + \frac{W_J}{2} \\ 0, & \text{otherwise} \end{cases} \quad (4)$$

where f_J and W_J represent the center frequency and bandwidth of PBI, respectively. $I(t)$ denotes Multiple Access Interference (MAI) for the user of interest.

C. INPUT OF ACQUISITION SYSTEM

Generation network for the input signal of MC-DS-CDMA acquisition system of the first user is depicted in Figure 2, and the signals at each point are presented in (5) and (6). In

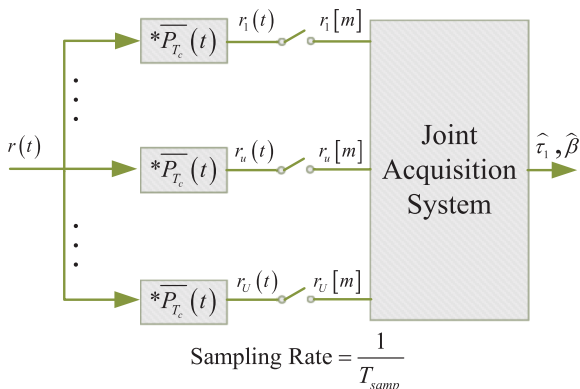


FIGURE 2. Generation network for the input signal of MC-DS-CDMA acquisition system of the first user.

order to ignore the adjacent channel interference, there is a Chip Pulse Matched-Filter (CPMF) whose impulse response is $P_{T_c}(t) = P_{T_c}(DT_c - t)$ adopted. And the output of CPMF for u th sub-channel is given in the form of

$$r_u(t) = \alpha_{1,u} \sqrt{\frac{P}{U}} \sum_{l=0}^{L-1} c_1(l) \psi_{T_c}(t - lT_c - \tau_1) \times \exp[j2\pi\beta(f_u + f_c)t + j\theta_{1,u}] + n_I(t) + n_w(t) + n_J(t) \quad (5)$$

where $\psi_{T_c}(t) \triangleq \int_{-\infty}^{+\infty} P_{T_c}(\tau_1) \overline{P_{T_c}}(\tau_1 - t) d\tau_1$ is a raised cosine waveform having a time-domain support range of $[0, 2DT_c)$. $n_w(t) \triangleq \int_{-\infty}^{+\infty} w(\tau_1) \overline{P_{T_c}}(\tau_1 - t) d\tau_1$ denotes the filtered noise; $n_J(t) \triangleq \int_{-\infty}^{+\infty} J(\tau_1) \overline{P_{T_c}}(\tau_1 - t) d\tau_1$ is the term of PBI interference $J(t)$ after passing through CPMF, while $n_I(t) \triangleq \int_{-\infty}^{+\infty} I(\tau_1) \overline{P_{T_c}}(\tau_1 - t) d\tau_1$ denotes the term of $I(t)$ after filtering. To accommodate the sampling rate ($\frac{1}{T_{samp}} = \frac{N}{T_c}$) of Analog-to-Digital Converter (ADC), $r_u(t)$ is supposed to be over-sampled, and the over-sampling ratio $N \in \mathbb{N}^+$ must be higher than 1. By stacking $M = NL$ samples of $r_u(t)$ over T_s , the following data sequence comprising M samples is given by

$$r_u[m] = \sum_{l=0}^{L-1} c_1(l) D_u[m] + n_I[m] + n_w[m] + n_J[m]$$

$$D_u[m] = \alpha_{1,u} \sqrt{\frac{P}{U}} \psi_{T_c}(mT_{samp} - lT_c - \tau_1) \times \exp[j2\pi\beta(f_u + f_c)mT_{samp} + j\theta_{1,u}] \quad (m = 0, 1, \dots, M-1) \quad (6)$$

where $n_I[m]$, $n_w[m]$ and $n_J[m]$ denote the sampling sequences of $n_I(t)$, $n_w(t)$ and $n_J(t)$, respectively. Note that $n_w[m]$ and $n_J[m]$ are both Gaussian by assumption, while $n_I[m]$ is asymptotically Gaussian with the sufficient condition on $\psi_{T_c}(t)$ (reported in APPENDIX A). In the next section, we will use (6) as the starting point of the proposed algorithm.

III. PROPOSED ALGORITHM

To exploit all the observations collected from sub-carriers for the coarse estimates of delay and Doppler factor, the two-dimensional joint acquisition algorithm is proposed in this discourse. Since there is no knowledge of carrier phase of the received signal in each sub-band, non-coherent sub-carrier combining scheme is considered in our proposed algorithm. Therefore, the process of estimating target parameters is equivalent to solve the problem provided in (7) when Equal Gain Combining (EGC) scheme is adopted.

$$Z(\tilde{\tau}_1, \tilde{\beta}) = \sum_{u=1}^U \left| \sum_{m=0}^{M-1} r_u[m] c(mT_{samp} - \tilde{\tau}_1) \times \exp[-j2\pi(f_u + f_c)\tilde{\beta}mT_{samp}] \right|^2 \quad (7)$$

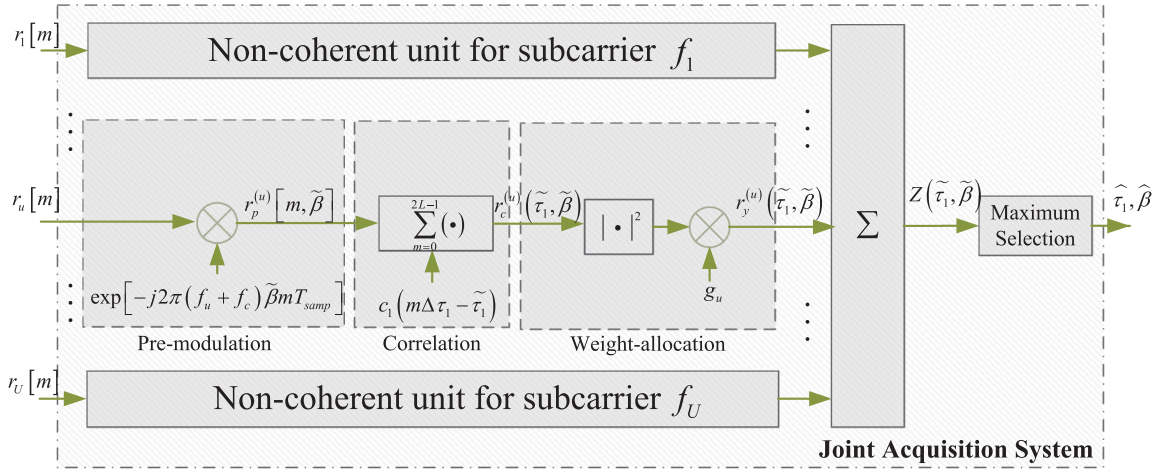


FIGURE 3. Block diagram of two-dimensional joint acquisition of delay and Doppler factor for MC-DS-CDMA.

where $\tilde{\tau}_1$ and $\tilde{\beta}$ denote the possible candidates of τ_1 and β , respectively. And the estimates of parameters we concerned are thereby obtained by

$$\{\hat{\tau}_1, \hat{\beta}\} = \underset{\{\tilde{\tau}_1, \tilde{\beta}\}}{\operatorname{argmax}} Z(\tilde{\tau}_1, \tilde{\beta}) \quad (8)$$

It is noted that the optimal ML solution $\{\hat{\tau}_1, \hat{\beta}\}$ claims for solving the optimization problem provided in (8), which is determined as a continuous two-dimensional brute search over $[0, T_s)$ and $[-\beta_{\max}, \beta_{\max})$, corresponding to the uncertain region of τ_1 and β , respectively. However, the computing complexity of this exhaustive search seems to be prohibitive. Hence a practical alternative with the aid of grid-based searching scheme is employed to access the sub-optimal solution. The block diagram of the proposed algorithm achieved by grid-based search is demonstrated in Figure 3, with the searching step sizes of τ_1 and β are $\Delta\tau_1 = \frac{T_c}{2}$ and $\Delta\beta = \frac{1}{T_s f_c}$, respectively.

Referring to Figure 3, there are five main phases in the proposed algorithm, including Pre-modulation, Correlation, Weight-allocation, Combining and Maximum Selection. Among them, Weight-allocation module serves as a calculation of combining weight with the aid of Adaptive Gain Control (AGC) technique, so that the following combining is able to counteract the adverse effect of PBI. Pre-modulation and Correlation modules are used to visit the possible candidates (predefined by searching grids) of Doppler factor and delay with observations collected from a single sub-carrier. Note that the estimated parameters τ_1 and β are the same for all sub-carriers in user k . Therefore, the outputs of Correlation module are capable to be combined and the maximum value would then be selected. The two-dimensional coordinates of maximum value index the sub-optimal ML estimates of τ_1 and β , respectively. The signals marked in block diagram can be expressed as (9) to (12).

$$\begin{aligned} r_p^{(u)}[m, \tilde{\beta}] &= r_u[m] \exp[-j2\pi(f_u + f_c)\tilde{\beta}mT_{samp}] + n[m] \\ &= \alpha_{1,u} \sqrt{\frac{P}{U}} B[m] \exp[j(2\pi(\beta - \tilde{\beta}) \\ &\quad \times (f_u + f_c)mT_{samp} + \theta_{1,u})] + n[m] \end{aligned}$$

$$B[m] = \sum_{l=0}^{L-1} c_l(l)\psi_{T_c}(mT_{samp} - lT_c - \tau_1) \quad (9)$$

$$\begin{aligned} r_c^{(u)}(\tilde{\tau}_1, \tilde{\beta}) &= \sum_{m=0}^{2L-1} r_p^{(u)}[m, \tilde{\beta}] c_l(m\Delta\tau_1 - \tilde{\tau}_1) + n(\tilde{\tau}_1) \\ &\approx \alpha_{1,u} A_{1,u} \exp(j\omega_{1,u}) + n(\tilde{\tau}_1) \\ A_{1,u} &= \sqrt{\frac{P}{U}} R(\tilde{\tau}_1) \operatorname{sinc}[(f_u + f_c)(\beta - \tilde{\beta})T_s] \\ \omega_{1,u} &= \pi(f_u + f_c)(\beta - \tilde{\beta})T_s + \theta_{1,u} \end{aligned} \quad (10)$$

$$\begin{aligned} r_y^{(u)}(\tilde{\tau}_1, \tilde{\beta}) &= g_u |r_c^{(u)}(\tilde{\tau}_1, \tilde{\beta})|^2 \\ &= g_u \left\{ \left[\operatorname{Re}(r_c^{(u)}(\tilde{\tau}_1, \tilde{\beta})) \right]^2 \right. \\ &\quad \left. + \left[\operatorname{Im}(r_c^{(u)}(\tilde{\tau}_1, \tilde{\beta})) \right]^2 \right\} \end{aligned} \quad (11)$$

$$Z(\tilde{\tau}_1, \tilde{\beta}) = \sum_{u=1}^U r_y^{(u)}(\tilde{\tau}_1, \tilde{\beta}) \quad (12)$$

where $R(\tilde{\tau}_1) = \frac{\cos[\frac{\lambda\pi}{T_c}(\tau_1 - \tilde{\tau}_1)]}{1 - [\frac{2\lambda}{T_c}(\tau_1 - \tilde{\tau}_1)]^2} \operatorname{sinc}[\frac{(\tau_1 - \tilde{\tau}_1)}{T_c}]$ denotes the correlation result of $B[m]$ and local PN code replica, and is defined as a unit-energy Root Raised Cosine (RRC) waveform with a roll-factor of λ . $n[m]$ and $n(\tilde{\tau}_1)$ are the noise terms in the output of Pre-modulator and Correlator, respectively, where $n(\tilde{\tau}_1)$ has zero mean and the variance of

$$\sigma_u^2 = \sigma_{n_w}^2 + \sigma_{n_l}^2 + \sigma_{n_j}^2 \quad (13)$$

where

$$\sigma_{n_w}^2 = \frac{\eta_o}{2} L \quad (14)$$

$$\sigma_{n_l}^2 = \frac{P(K-1)L}{2U} \left(1 - \frac{\lambda}{4}\right) \quad (15)$$

$$\begin{aligned} \sigma_{n_j}^2 &= \frac{L}{2} \int_{-\infty}^{\infty} [S_J(f - (f_c + f_u)) \\ &\quad + S_J(f + (f_c + f_u))] X(f) df \end{aligned} \quad (16)$$

where $X(f)$ is the Fourier transform of $\psi_{T_c}(t)$; $g_u = \frac{1}{P_r}$ is the AGC coefficient of u th branch, and would be omitted if there is no PBI existing. It is noted that P_r denotes the received signal power of u th branch, and has

$$P_r = \frac{\eta_o}{2} + \frac{PK}{2U} \left(1 - \frac{\lambda}{4} \right) + \frac{1}{2} \int_{-\infty}^{\infty} [S_J(f - (f_c + f_u)) + S_J(f + (f_c + f_u))] X(f) df \quad (17)$$

IV. PERFORMANCE ANALYSIS

In this passage, detection and estimation performance of the two-dimensional joint acquisition algorithm for MC-DS-CDMA would be explored. And the corresponding criteria of interest are detection probability and MSE values of delay and Doppler factor.

A. DETECTION PROBABILITY

To determine the detection probability of proposed algorithm for MC-DS-CDMA, we first develop the Probability Density Function (PDF) of $Z(\tilde{\tau}_1, \tilde{\beta})$. Assuming H_1 represents the case that there is a signal in a searching cell while H_0 denotes the other cases, the mean value and variance of $r_c^{(u)}(\tilde{\tau}_1, \tilde{\beta})$ under H_0 and H_1 are

$$H_0 : \begin{cases} \mu_0 \left[\text{Re} \left[r_c^{(u)}(\tilde{\tau}_1, \tilde{\beta}) \right] \right] = 0; \\ \mu_0 \left[\text{Im} \left[r_c^{(u)}(\tilde{\tau}_1, \tilde{\beta}) \right] \right] = 0; \\ \sigma_0^2 = \frac{1}{2} \text{var} \left[r_c^{(u)}(\tilde{\tau}_1, \tilde{\beta}) \right] = \frac{1}{2} \sigma_u^2; \end{cases} \quad (18)$$

$$H_1 : \begin{cases} \mu_1 \left[\text{Re} \left[r_c^{(u)}(\tilde{\tau}_1, \tilde{\beta}) \right] \right] = \alpha_{1,u} A_{1,u} \cos(\omega_{1,u}); \\ \mu_1 \left[\text{Im} \left[r_c^{(u)}(\tilde{\tau}_1, \tilde{\beta}) \right] \right] = \alpha_{1,u} A_{1,u} \sin(\omega_{1,u}); \\ \sigma_1^2 = \frac{1}{2} \text{var} \left[r_c^{(u)}(\tilde{\tau}_1, \tilde{\beta}) \right] = \frac{1}{2} \sigma_u^2; \end{cases} \quad (19)$$

Note that the conditional PDF of $r_y^{(u)}(\tilde{\tau}_1, \tilde{\beta})$ conditioned on $\alpha_{1,u}$ and H_i ($i = 0, 1$) obeys Chi-square distribution [20] with two degrees of freedom, then we have

$$P \left[r_y^{(u)} | \alpha_{1,u}; H_i \right] = \frac{1}{2g_u \sigma_u^2} \exp \left(-\frac{r_y^{(u)} + g_u \alpha_{1,u}^2 A_{1,u}^2}{2g_u \sigma_u^2} \right) \times I_0 \left(\frac{\alpha_{1,u} A_{1,u}}{\sigma_u^2} \sqrt{\frac{r_y^{(u)}}{g_u}} \right), \quad r_y^{(u)} \geq 0 \quad (20)$$

where $I_0(\cdot)$ is the zeroth-order-modified Bessel function. Therefore, for AWGN scenario ($\alpha_{1,u} = 1$), the PDF of $r_y^{(u)}(\tilde{\tau}_1, \tilde{\beta})$ conditioned on H_i is described as

$$P \left[r_y^{(u)}; H_i \right] = \frac{1}{2g_u \sigma_u^2} \exp \left(-\frac{r_y^{(u)} + g_u A_{1,u}^2}{2g_u \sigma_u^2} \right) \times I_0 \left(\frac{A_{1,u}}{\sigma_u^2} \sqrt{\frac{r_y^{(u)}}{g_u}} \right), \quad r_y^{(u)} \geq 0 \quad (21)$$

And in the Rayleigh fading case, the PDF of $r_y^{(u)}(\tilde{\tau}_1, \tilde{\beta})$ conditioned on H_i could be derived by substituting (20) and

the PDF of $\alpha_{1,u}$, which is given by

$$P \left[r_y^{(u)}; H_i \right] = \int_0^{\infty} P(\alpha_{1,u}) P \left[r_y^{(u)} | \alpha_{1,u}; H_i \right] d\alpha_{1,u} = \frac{1}{g_u (A_{1,u}^2 + 2\sigma_u^2)} \exp \left[-\frac{r_y^{(u)}}{g_u (A_{1,u}^2 + 2\sigma_u^2)} \right], \quad r_y^{(u)} \geq 0 \quad (22)$$

where $P(\alpha_{1,u})$ denotes the PDF of $\alpha_{1,u}$, and is defined as

$$P(\alpha_{1,u}) = 2\alpha_{1,u} \exp(-\alpha_{1,u}^2) \quad (23)$$

Therefore, the PDF of $Z(\tilde{\tau}_1, \tilde{\beta})$ conditioned on H_i could be calculated by the following formula chain from (24) to (25) for AWGN case, and (26) to (27) for the Rayleigh fading counterpart.

$$\begin{aligned} \phi_{r_y^{(u)} | H_i}(s) &= \int_0^{\infty} \exp(sr_y^{(u)}) P \left[r_y^{(u)}; H_i \right] dr_y^{(u)} \\ &= \frac{1}{1 - 2g_u \sigma_u^2 s} \exp \left(\frac{g_u A_{1,u}^2 s}{1 - 2g_u \sigma_u^2 s} \right) \end{aligned} \quad (24)$$

$$\begin{aligned} P[Z; H_i] &= \frac{1}{2\pi j} \oint \exp(-sZ) \prod_{u=1}^U \phi_{r_y^{(u)} | H_i}(s) ds \\ &= \frac{1}{2\pi j} \oint \frac{1}{\prod_{u=1}^U (1 - 2g_u \sigma_u^2 s)} \\ &\quad \times \exp \left(-sZ + \sum_{u=1}^U \left(\frac{g_u A_{1,u}^2 s}{1 - 2g_u \sigma_u^2 s} \right) \right) ds \end{aligned} \quad (25)$$

$$\begin{aligned} \phi_{r_y^{(u)} | H_i}(s) &= \int_0^{\infty} \exp(sr_y^{(u)}) P \left[r_y^{(u)}; H_i \right] dr_y^{(u)} \\ &= \frac{1}{1 - g_u (A_{1,u}^2 + 2\sigma_u^2) s} \end{aligned} \quad (26)$$

$$\begin{aligned} P[Z; H_i] &= \frac{1}{2\pi j} \oint \exp(-sZ) \prod_{u=1}^U \phi_{r_y^{(u)} | H_i}(s) ds \\ &= - \sum_{u=1}^U \frac{\left[g_u (A_{1,u}^2 + 2\sigma_u^2) \right]^{U-2} \exp \left(-\frac{Z}{g_u (A_{1,u}^2 + 2\sigma_u^2)} \right)}{\prod_{i=1, i \neq u}^U \left[g_u (A_{1,u}^2 + 2\sigma_u^2) - g_i (A_{1,i}^2 + 2\sigma_i^2) \right]} \end{aligned} \quad (27)$$

It is noted that the integration result of (25) is tough to obtain precisely since the complicated nature of the exponential factor. To circumvent this problem, we define σ_L^2 and

σ_U^2 as the variances of noise components of correlator output when there is PBI and there is no PBI respectively. Therefore, the upper bound of detection probability could be obtained when $\sigma_u^2 = \sigma_U^2$, and the corresponding g_u can be derived from (17) with the absence of PBI. While the lower bound is derived in the case of $\sigma_u^2 = \sigma_L^2$. Under this assumption, (25) can be converted into (28) with the aid of residue theorem and (24).

$$\begin{aligned}
 P[Z; H_i] &= \frac{1}{2\pi j} \oint \frac{1}{(1 - 2g_u\sigma_u^2 s)^U} \exp\left(-sZ + \frac{\sum_{u=1}^U g_u A_{1,u}^2 s}{1 - 2g_u\sigma_u^2 s}\right) ds \\
 &= \frac{1}{2g_u\sigma_u^2} \left(\frac{Z}{\sum_{u=1}^U g_u A_{1,u}^2}\right)^{\frac{U-1}{2}} \exp\left(-\frac{Z + \sum_{u=1}^U g_u A_{1,u}^2}{2g_u\sigma_u^2}\right) \\
 &\quad \times I_{U-1}\left(\frac{1}{g_u\sigma_u^2} \sqrt{Z \sum_{u=1}^U g_u A_{1,u}^2}\right) \quad (28)
 \end{aligned}$$

The detection probability is determined as the chance that the largest of the decision variable Z ($\tilde{\tau}_1, \tilde{\beta}$) associating with $N_{grid} = \frac{2\beta_{max}}{\Delta\beta} \times 2L$ cells corresponds to the correct estimate of τ_1 and β [16]. Hence, the detection probability is provided as

$$P_d = \int_0^\infty P[Z; H_1] \left[\int_0^Z P[x; H_0] dx \right]^{N_{grid}-1} dZ \quad (29)$$

The remaining integrations of (29) for these two channel cases have been done numerically.

B. MEAN SQUARE ERROR

Given estimation error would occur when the largest of the decision variable associating with N_{grid} cells arises in the case of H_0 , the MSE values of Doppler factor and delay could be described with the aid of the probability of error. Defining Q_0 and Q_1 as the decision variable values of H_0 and H_1 respectively, then the probability of Q_0 overtopping Q_1 is provided as

$$P_T = \int_{-\infty}^1 \left[\int_0^\infty P_{Z;H_1}(ty) P_{Z;H_0}(y) y dy \right] dt \quad (30)$$

For the case of AWGN, P_T is the Cumulative Distribution Function (CDF) of non-central F distribution [20] with $2U$ degrees of freedom for both numerator and denominator upon substituting (28) into (30), and is thereby shown as

$$P_T = \int_{-\infty}^1 \exp\left(-\frac{\sum_{u=1}^U g_u A_{1,u}^2}{2g_u\sigma_u^2}\right) \sum_{p=0}^\infty \frac{1}{p!}$$

$$\times \left(\frac{\sum_{u=1}^U g_u A_{1,u}^2}{2g_u\sigma_u^2} \right)^p \frac{t^{U+p-1}}{B(U+p, U)} (1+t)^{-2U-p} dt \quad (31)$$

where $B(U+p, U) = \frac{\Gamma(U+p)\Gamma(U)}{\Gamma(2U+p)}$ denotes Beta function with $\Gamma(\cdot)$ representing Gamma function. The remaining integration has been done numerically. And P_T for Rayleigh fading scenario can be obtained in the similar way by substituting (27) into (30). We now assume the probability of Q_0 overtopping Q_1 for all the candidates in H_0 is the same, then the MSE values of Doppler factor and delay could be given by

$$\begin{aligned}
 MSE_{Df} &= P_T E_{total}^{2(Df)} \\
 MSE_{Delay} &= P_T E_{total}^{2(Delay)} \quad (32)
 \end{aligned}$$

where $E_{total}^{2(Df)}$ and $E_{total}^{2(Delay)}$ denote the sums of squares of all the possible error values for Doppler factor and delay respectively in grid-based searching process.

V. NUMERICAL RESULTS

A. SIMULATION SYSTEM SET UP AND PERFORMANCE METRICS

The performance analysis of the proposed algorithm has been developed in Section IV. In this discourse, we will conduct verifications of previous deduction numerically, and develop performance comparison with the existing single-carrier system. The primary performance criteria concerned here include the detection probability (namely P_d) as well as the MSE of Doppler factor and delay. Note that the estimates of β and τ_1 are deemed as ‘‘correct’’ only when the corresponding estimation errors have absolute value less than the corresponding searching step sizes. The system parameters adopted in our simulations are the common choices of LEO satellite communication systems that provide global real-time personal communication services [21], and are listed in Table 1. For a fair comparison, we assume the total bandwidth of single-carrier system is equal to that of MC-DS-CDMA system, which implies that the spreading gain of MC-DS-CDMA system using U sub-carriers is a factor of U lower than that of the corresponding single-carrier system, and the chip period of sub-carrier satisfies $T_c = UT_c^{(SC)}$.

TABLE 1. System parameters of simulation.

Symbol	Quantity	Value
λ	Roll-factor	0.35
T_s	Symbol period	0.2ms
L_{SC}	Spreading gain of single-carrier system	10240
$T_c^{(SC)}$	Chip period of single-carrier system	19.5ns
f_c	Radio frequency	2GHz

Under assumption that the uncertainty ranges of Doppler factor and delay are $[-2.5 \times 10^{-5}, 2.5 \times 10^{-5}]$ and $[0, T_s)$

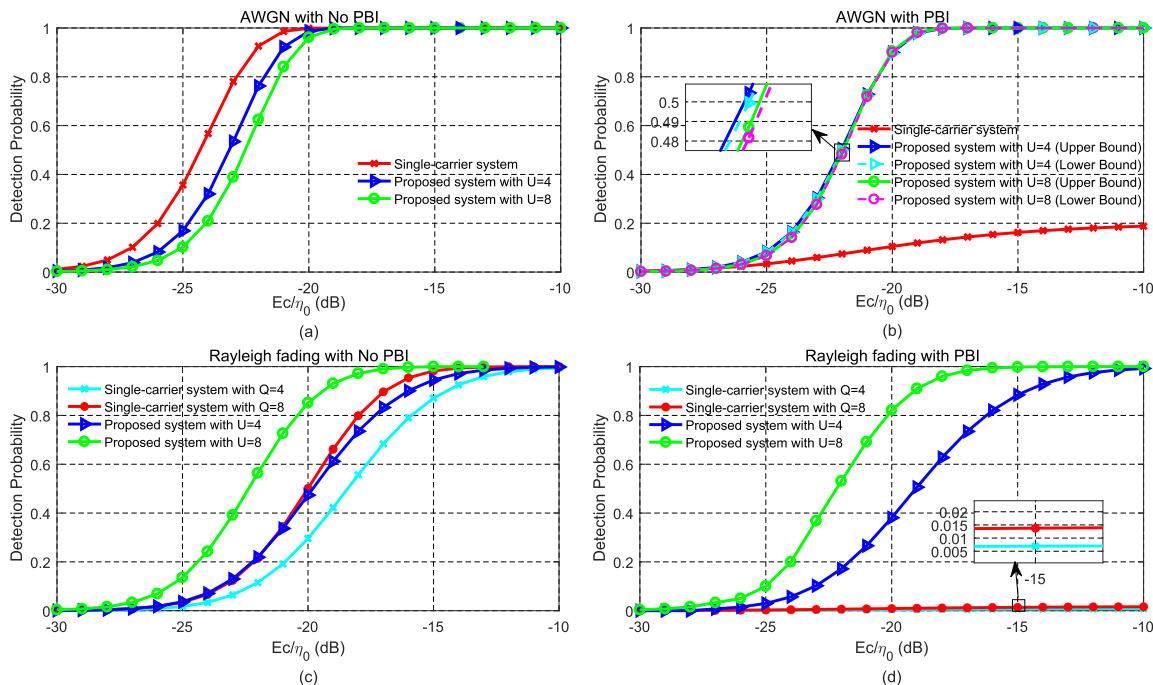


FIGURE 4. Detection probability versus E_c/η_0 when $K = 1$ in terms of AWGN and Rayleigh fading channels, performance comparison of single-carrier system and two-dimensional joint acquisition algorithm for MC-DS-CDMA system, computed from (45) and (29) respectively.

respectively, with $\frac{1}{T_s f_c}$ and $\frac{T_c^{(SC)}}{2}$ being the corresponding searching step sizes, the total number of searching grids for single-carrier system would be equal to 430080, and that of two-dimensional joint acquisition of MC-DS-CDMA is thereby satisfying $N_{grid} = \frac{430080}{U}$. It is also noted that the uncertainty range of Doppler factor is derived from the case that satellite elevation equals to 780km [21], and our simulations are conducted at the worst case of Doppler factor and delay, which means the true values of β and τ_1 fall just at the middle of two neighboring searching grids.

B. EVALUATION OF DETECTION PROBABILITY

The detection probabilities of proposed algorithm under different E_c/η_0 in both AWGN and Rayleigh fading cases are reported in Figure 4 when $K = 1$, together with the discussion of the existence of PBI. As a comparison, detection performance of single-carrier system with equivalent simulation parameters is also provided. The results appearing in Figure 4 (a) and (c) are generated when there is no PBI. For all these, it is apparent to see the detection probabilities of systems in AWGN scenario outperform those in Rayleigh fading case. Besides, it is also observed that in AWGN channel, the detection probability of proposed algorithm for MC-DS-CDMA is inferior to that of its single-carrier counterpart. And the probability would keep worsening as the increase in the number of sub-carriers (U) since there is no frequency diversity gain, but has Signal-to-Noise Ratio (SNR) loss due to the non-coherent equal gain combining. However, things are quite different when we project the light on Rayleigh

fading case, where the detection probability of proposed algorithm for MC-DS-CDMA remains rising when U increases, and is always superior to that of its single-carrier counterpart. It is also presented that in Rayleigh fading channel the performance gap between the proposed system and its single-carrier counterpart would be narrowed when U decreases. Therefore, when it comes to the case that PBI is absent, the proposed algorithm for MC-DS-CDMA is capable to present superior detection performance to its single-carrier counterpart in Rayleigh fading channel.

The influence of PBI on detection probabilities in both AWGN and Rayleigh fading channels are depicted in Figure 4 (b) and (d), respectively, with $f_j = f_1 + f_c$, $W_j = \frac{1+\lambda}{T_c}$ and $JSR = 10 \log \left(\frac{W_j \eta_j}{U E_c / T_c} \right) = 26dB$. The detection probability in AWGN case is described by its upper and lower bounds, and these two bounds are shown to be rather tight when the adverse effect of PBI is small comparing to the effects of noise and MAI. It should be noted that the detection performance gap between the cases of $U = 4$ and $U = 8$ is narrowed in AWGN channel. On the contrary, this performance gap is observed to be wider in Rayleigh fading channel. This implies the adverse effect caused by PBI contributes more in MC-DS-CDMA system with fewer sub-carriers though AGC technique is employed. Moreover, We can also observe that for both channel cases, the degradation incurred by PBI is much more severe in single-carrier system than in proposed algorithm for MC-DS-CDMA, and the detection probability of single-carrier system would not improve though the number

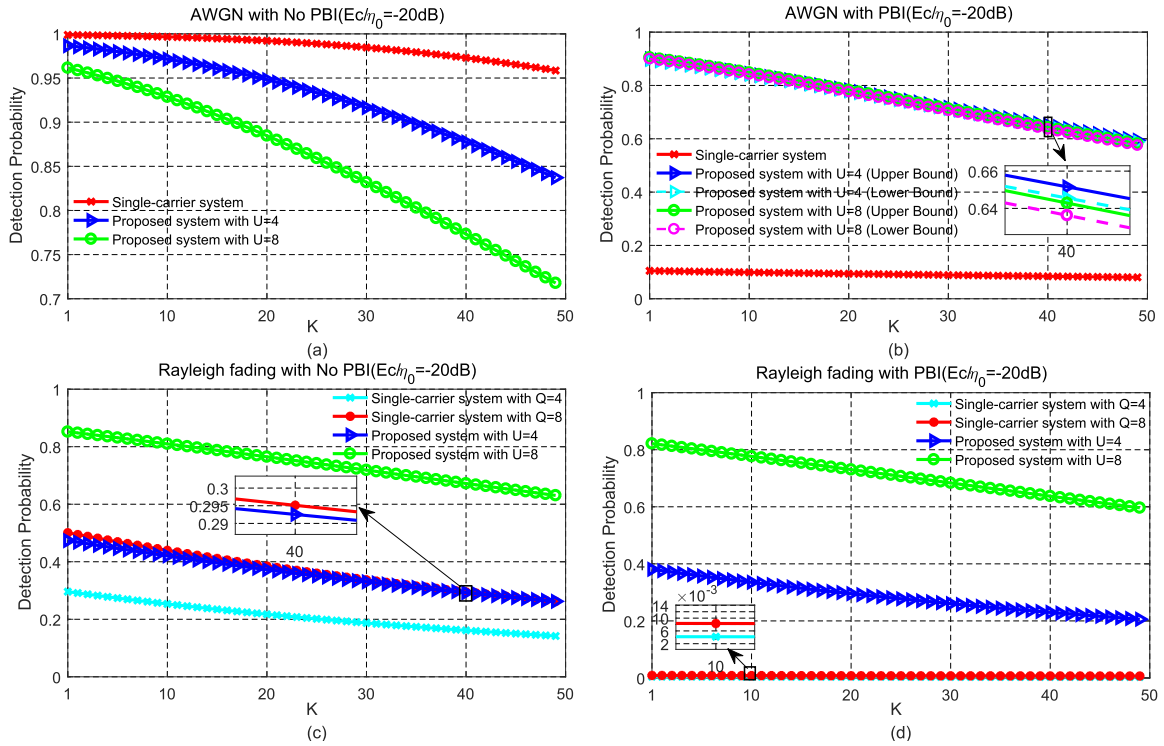


FIGURE 5. Detection probability versus the number of users K when $E_c/\eta_0 = -20\text{dB}$ in terms of AWGN and Rayleigh fading channels, performance comparison of single-carrier system and two-dimensional joint acquisition algorithm for MC-DS-CDMA system, computed from (45) and (29) respectively.

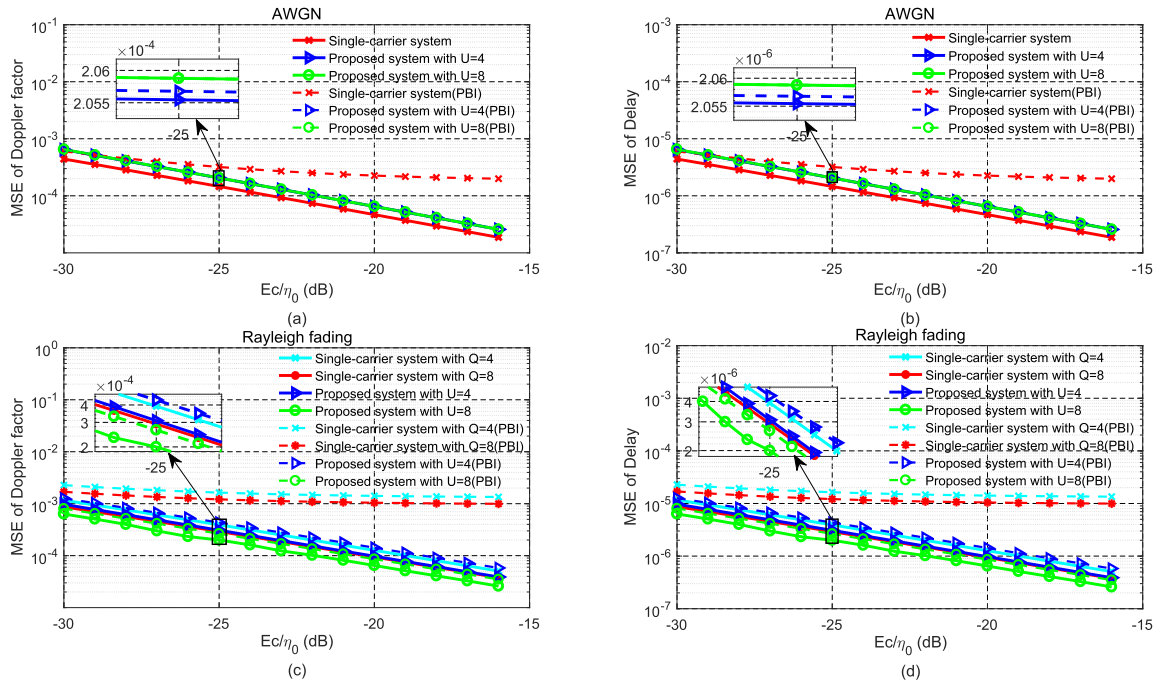


FIGURE 6. MSE of Doppler factor (normalized by $(1/2T_s f_c)^2$) and delay (normalized by T_s^2) versus E_c/η_0 when $K = 1$ in terms of AWGN and Rayleigh fading channels, performance comparison of single-carrier system and two-dimensional joint acquisition algorithm for MC-DS-CDMA system, computed from (47) and (32) respectively.

of resolvable paths increases in terms of Rayleigh fading channel. Thus, conclusion could be drawn that the detection probability of proposed algorithm for MC-DS-CDMA

is advantageous comparing to its single-carrier counterpart when PBI is present. However, it is predictable that same detection performance would be achieved by proposed

system and its single-carrier counterpart when PBI spans all the sub-carriers.

Figure 5 is dedicated to show the detection probabilities versus the number of users (K), when $E_c/\eta_0 = -20dB$ in terms of two types of channel mentioned above. As expected, the detection probabilities of both single-carrier and proposed system suffer degradation as the increase in K not only in AWGN channel but in Rayleigh fading case as well. However, the detection probability in AWGN channel remains superior with respect to that of Rayleigh fading channel, though quite opposite trends have been followed by the detection probabilities of previous two channels as the increase in U .

C. EVALUATION OF MEAN SQUARE ERROR

Figure 6 focuses on the MSE values of Doppler factor and delay for proposed system with single-carrier system serving as a contrast, when both AWGN and Rayleigh fading channels are considered. Apparently, when PBI is absent, MSE values of Doppler factor and delay are observed to be more superior as the decrease in U in the former channel case, as a consequence, optimal performance would be achieved by single-carrier system ($U = 1$). On the contrary, advantageous MSE performance of Doppler factor and delay are provided when U increases in Rayleigh fading scenario, and slight improvement can also be seen in single-carrier system when the number of resolvable paths (Q) increases. The presence of PBI brings MSE performance deterioration for both MC-DS-CDMA and single-carrier systems in AWGN and Rayleigh fading channels, by contrast, the MSE performance of Doppler factor and delay in proposed system are proved to be better with respect to its single-carrier counterpart not only in AWGN case but in Rayleigh fading channel as well. Therefore, the MC-DS-CDMA system with proposed algorithm has advantageous MSE performance in Rayleigh fading channel and the case that PBI presents comparing with its single-carrier counterpart.

VI. CONCLUSION

In this article, we have conceived a two-dimensional joint acquisition algorithm for MC-DS-CDMA in consideration of LEO satellite systems in urban areas in presence of multi-path, Doppler shift and PBI. In the proposed algorithm, the acquisition process of delay and Doppler factor is equivalent to find the ML solution of decision variable falling into two-dimensional uncertain region of the estimated parameters. Given the formidable computing complexity of brute-force search, in this article, grid-based search scheme is concerned to acquire the sub-optimal ML estimates of delay and Doppler factor. In order to evaluate the detection and estimation performance of the proposed algorithm, the detection probability and MSE performance of delay and Doppler factor are explored by comparing with its single-carrier counterpart in both AWGN and Rayleigh fading cases. As a consequence, the MC-DS-CDMA with proposed two-dimensional joint acquisition algorithm is superior to its single-carrier counterpart in Rayleigh fading channel. Thanks to the gain of

frequency diversity, this advantage would be more significant when the number of sub-carriers increases. Besides, for both channel cases, the MC-DS-CDMA with proposed algorithm is expected to be more robust to PBI comparing with its single-carrier counterpart.

APPENDIX A SUFFICIENT CONDITION FOR THE GAUSSIAN APPROXIMATION

We now shed light on the deduction of the sufficient condition for the Gaussian approximation of $n_I[m]$. Recalling (6), $n_I[m]$ could be modeled as

$$n_I[m] = \sqrt{\frac{P}{U}} \sum_{k=2}^K n_I^{(k)}[m]$$

$$n_I^{(k)}[m] = \sum_{m=-\infty}^{\infty} a_m^{(k)} \psi_{T_c}(mT_{samp} - \tau_k) \quad (33)$$

where $a_m^{(k)}$ is an independent random binary sequence. Assuming $a_m^{(k)}$ and τ_k are independent for different user, $n_I^{(k)}[m]$ ($k = 1, 2, \dots, K$) is independent and would be asymptotically Gaussian by the Liapounoff version of the central limit theorem if its third absolute central moment is finite [22]. Therefore, the upper bound of the third absolute moment of $n_I^{(k)}[m]$ is given by

$$E \left| n_I^{(k)}[m] \right|^3 = E \left| \sum_{m=-\infty}^{\infty} a_m^{(k)} \psi_{T_c}(mT_{samp} - \tau_k) \right|^3$$

$$\leq E \left\{ \sum_{m=-\infty}^{\infty} \left| a_m^{(k)} \psi_{T_c}(mT_{samp} - \tau_k) \right| \right\}^3$$

$$= E \left\{ \sum_{m=-\infty}^{\infty} \left| \psi_{T_c}(mT_{samp} - \tau_k) \right| \right\}^3 \quad (34)$$

Hence, a sufficient condition for the Gaussian approximation of $n_I[m]$ for all possible τ_k would be

$$\sum_{m=-\infty}^{\infty} \left| \psi_{T_c}(mT_{samp} - \tau_k) \right| < \infty \quad (35)$$

APPENDIX B DETECTION PROBABILITY OF SINGLE-CARRIER SYSTEM

To facilitate the performance comparison of band-limited single-carrier CDMA acquisition system and the MC-DS-CDMA acquisition system with proposed algorithm, the detection probability of single-carrier CDMA acquisition system is developed in this part. For fair comparison, we assume the total bandwidth and transmitted power of single-carrier system are equal to those of MC-DS-CDMA system. The spreading gain of single-carrier system satisfies $L_{SC} = UL$, where L denotes the spreading gain of multi-carrier system. The system parameters adopted in single-carrier system are listed in Table 1. Besides, it is also noted that the number of resolvable paths Q for single-carrier system satisfies $Q = U$ for all users, and the self-interference

caused by multi-path is ignored in this discourse. Therefore, the CIR of single-carrier CDMA acquisition system matched to user k is defined as

$$h_k(t) = \sum_{q=1}^Q \alpha_{k,q} \delta \left[(1 + \beta)t - qT_c^{(SC)} \right] \exp(-j\varphi_{k,q}) \quad (36)$$

where $\alpha_{k,q}$ and $\varphi_{k,q}$ are independently Rayleigh random variables with the second moment of $\frac{1}{Q}$ [15], IID uniform random variables over $[0, 2\pi)$, respectively. Apparently, these two variables should be both omitted when AWGN channel is considered. Regarding the first user as the user of interest, then the received signal of single-carrier system is provided as

$$\begin{aligned} r_{SC}(t) &= \sum_{q=1}^Q \alpha_{1,q} \sqrt{P_{SC}} c_1^{(SC)} \left(t - qT_c^{(SC)} - \tau_1 \right) \\ &\quad \times \exp(j2\pi\beta f_c t + j\theta_{1,q}) + I_{SC}(t) + w(t) + J(t) \\ I_{SC}(t) &= \sum_{k=2}^K \sum_{q=1}^Q \alpha_{k,q} \sqrt{P_{SC}} b_k \left(t - qT_c^{(SC)} - \tau_k \right) \\ &\quad \times c_k^{(SC)} \left(t - qT_c^{(SC)} - \tau_k \right) \exp(j2\pi\beta f_c t + j\theta_{k,q}) \end{aligned} \quad (37)$$

where P_{SC} denotes the transmitted power of single-carrier system; $\theta_{k,q} = 2\pi\beta f_c \tau_k + \theta_t - \theta_r - \varphi_{k,q}$ is the random phase which is uniformly distributed over $[0, 2\pi)$; $c_k^{(SC)}(t) = \sum_{l=0}^{L_{SC}-1} c_k^{(SC)}(l) P_{T_c^{(SC)}}(t - lT_c^{(SC)})$ denotes the signature waveform of k th user, where $T_c^{(SC)} = \frac{T_s}{L_{SC}}$ is the chip period, and $c_k^{(SC)}(l)$ is the PN spreading sequence with $c_k^{(SC)}(l) \in \{-1, 1\}$. Here we use $P_{T_c^{(SC)}}(t)$ denoting the impulse response of the bandlimited CPSF of single-carrier system, which is typically a unit-energy Square Root Raised Cosine (SRRC) waveform having a roll-factor of λ and time-supported over the interval of $[0, DT_c^{(SC)})$ with $D \in \{1, 2, 3, \dots\}$ and $2D \leq L_{SC}$. In order to ensure the system complexity is the same as that of multi-carrier system, it is assumed that U correlators are adopted for parallel search in single-carrier system, and the outputs of all branches are approximately independently distributed [23]. Therefore, following the similar deduction of multi-carrier system, the conditional PDF of decision variable Z_q ($q = 1, 2, \dots, Q$) conditioned on $\alpha_{1,q}$ and H_i ($i = 0, 1$) obeys Chi-square distribution with two degrees of freedom, and is given by

$$\begin{aligned} P[Z_q | \alpha_{1,q}; H_i] &= \frac{1}{2\sigma_{SC}^2} \exp\left(-\frac{Z_q + \rho}{2\sigma_{SC}^2}\right) \\ &\quad \times I_0\left(\frac{\sqrt{\rho Z_q}}{\sigma_{SC}^2}\right), \quad Z_q \geq 0 \end{aligned} \quad (38)$$

where ρ denotes the non-central parameter, and is defined as

$$\begin{aligned} \rho &= \left(\alpha_{1,q} \sqrt{P_{SC}} R(\tilde{\tau}_1) \operatorname{sinc} \left[f_c (\beta - \tilde{\beta}) T_s \right] \right)_{A_{1,q}}^2 \\ R(\tilde{\tau}_1) &= \frac{\cos \left[\frac{\lambda\pi}{T_c^{(SC)}} (\tau_1 - \tilde{\tau}_1) \right]}{1 - \left[\frac{2\lambda}{T_c^{(SC)}} (\tau_1 - \tilde{\tau}_1) \right]^2} \operatorname{sinc} \left[\frac{(\tau_1 - \tilde{\tau}_1)}{T_c^{(SC)}} \right] \end{aligned} \quad (39)$$

σ_{SC}^2 denotes the variance under H_1 and H_0 conditions, and is given by

$$\sigma_{SC}^2 = \sigma_w^2 + \sigma_I^2 + \sigma_J^2 \quad (40)$$

where

$$\sigma_w^2 = \frac{\eta_0}{2} L_{SC} \quad (41)$$

$$\sigma_I^2 = \frac{P_{SC} (K - 1) L_{SC}}{2} \left(1 - \frac{\lambda}{4} \right) \quad (42)$$

$$\begin{aligned} \sigma_J^2 &= \frac{L_{SC}}{2} \int_{-\infty}^{\infty} [S_J(f - f_c) + S_J(f + f_c)] \\ &\quad \times X'(f) df \end{aligned} \quad (43)$$

where $X'(f)$ is the Fourier transform of $\psi_{T_c^{(SC)}}(t)$. For AWGN case, the PDF of Z_q conditioned on H_i could be available by substituting $\alpha_{1,q} = 1$ into (38) and (39), then the detection probability would be obtained with the aid of (29). However, when it comes to the scenario of Rayleigh fading, the PDF of Z_q conditioned on H_i is

$$\begin{aligned} P[Z_q; H_i] &= \int_0^{\infty} P(\alpha_{1,q}) P[Z_q | \alpha_{1,q}; H_i] d\alpha_{1,q} \\ &= \frac{1}{\frac{A_{1,q}^2}{Q} + 2\sigma_{SC}^2} \exp\left[-\frac{Z_q}{\frac{A_{1,q}^2}{Q} + 2\sigma_{SC}^2}\right] \end{aligned} \quad (44)$$

Note that there is more than one correct estimate of τ_1 and β existing in single-carrier system due to the resolvable multipath. Therefore, the detection probability of single-carrier system in Rayleigh fading channel is determined as the probability that the largest of decision variable corresponds to one of the Q correct paths, and is presented as

$$\begin{aligned} P_d &= Q \int_0^{\infty} P[Z_q; H_1] \left[\int_0^{Z_q} P[x; H_0] dx \right]^{UN_{grid}-Q} \\ &\quad \times \left[\int_0^{Z_q} P[y; H_1] dy \right]^{Q-1} dZ_q \end{aligned} \quad (45)$$

The remaining integration of (45) has been done numerically.

APPENDIX C MEAN SQUARE ERROR OF SINGLE-CARRIER SYSTEM

Analysis of MSE for single-carrier acquisition system is recorded in this part. We first look at the case of AWGN, in which the estimation error occurs when the largest of

the decision variable associating with UN_{grid} cells appears in H_0 . Then the MSE values of Doppler factor and delay could be described with the aid of the probability of Q_0 overtopping Q_1 , assuming Q_0 and Q_1 are the decision variable values of H_0 and H_1 , respectively. Observing the probability of interest P_T for single-carrier system obeys non-central F distribution with 2 degrees of freedom for both numerator and denominator, we have

$$P_T = \int_{-\infty}^1 \left[\int_0^{\infty} P_{Z_q;H_1}(ty) P_{Z_q;H_0}(y) y dy \right] dt \\ = \int_{-\infty}^1 \exp\left(-\frac{\rho}{2\sigma_{SC}^2}\right) \sum_{p=0}^{\infty} \frac{1}{p!} \\ \times \left(\frac{\rho}{2\sigma_{SC}^2}\right)^p \frac{t^p}{B(1+p, 1)} (1+t)^{-2-p} dt \quad (46)$$

where $B(1+p, 1) = \frac{\Gamma(1+p)\Gamma(1)}{\Gamma(2+p)}$ denotes Beta function with $\Gamma(\cdot)$ representing Gamma function. ρ is defined in (39) with $\alpha_{1,q} = 1$. The remaining integration has been done numerically. In terms of Rayleigh fading scenario, there is more than one correct estimate of τ_1 and β in single-carrier system due to the resolvable multi-path. Therefore, estimation error happens when the largest of decision variable fails to correspond to any correct paths. Then the probability of Q_0 overtopping Q_1 can be obtained in the similar way by substituting (44) into (30). Assuming the probability of Q_0 overtopping Q_1 for all the candidates in H_0 is the same, the MSE values of Doppler factor and delay could be calculated as

$$MSE_{Df}^{(SC)} = P_T E_{(SC)}^{2(Df)} \\ MSE_{Delay}^{(SC)} = P_T E_{(SC)}^{2(Delay)} \quad (47)$$

where $E_{(SC)}^{2(Df)}$ and $E_{(SC)}^{2(Delay)}$ denote the sums of squares of all the possible error values for Doppler factor and delay respectively in grid-based searching process. Notedly, $E_{(SC)}^{2(Df)}$ and $E_{(SC)}^{2(Delay)}$ is associated with $UN_{grid} - 1$ cells for AWGN case, while is only related to $UN_{grid} - Q$ cells in its Rayleigh fading counterpart.

REFERENCES

- [1] R. Cochetti, "Low earth orbit (LEO) mobile satellite communications systems," in *linear Networks and Systems*, 1st ed. Boston, MA, USA: World Scientific, 2014, pp. 119–156.
- [2] J. Foust, "SpaceX's space-Internet woes: Despite technical glitches, the company plans to launch the first of nearly 12,000 satellites in 2019," *IEEE Spectr.*, vol. 56, no. 1, pp. 50–51, Jan. 2019.
- [3] B. Chapman, S. Hensley, Y. Lou, B. Hawkins, R. Muellerschoen, and T. Michel, "Analysis of multi-aspect and fully polarimetric L-band SAR data from uavsar over spacex rocket debris site," in *Proc. IGARSS. Conf.*, Jul. 2017, pp. 3294–3296.
- [4] J. Radtke, C. Keschull, and E. Stoll, "Interactions of the space debris environment with mega constellations—Using the example of the OneWeb constellation," *Acta Astronaut.*, vol. 131, no. 2, pp. 55–68, Feb. 2017.
- [5] B. Vucetic and J. Du, "Channel modeling and simulation in satellite mobile communication systems," *IEEE J. Sel. Areas Commun.*, vol. 10, no. 8, pp. 1209–1218, Oct. 1992.
- [6] B. R. Vojcic, L. B. Milstein, and R. L. Pickholtz, "Downlink DS CDMA performance over a mobile satellite channel," *IEEE Trans. Veh. Technol.*, vol. 45, no. 3, pp. 551–560, Aug. 1996.

- [7] L. L. Yang, "Principles of Multicarrier communications," in *Multicarrier Communications*. 1st ed. West Sussex, U.K.: Wiley, 2009, pp. 97–151.
- [8] S. D. Paul, S. Asif, and S. P. Majumder, "Performance analysis of a MC-DS-CDMA wireless communication system with RAKE receiver over a Rayleigh fading channel with receive diversity," in *Proc. IEEE ICECE Conf.*, Dec. 2012, pp. 178–181.
- [9] K. Wu, P. C. Cosman, and L. B. Milstein, "Multicarrier DS-CDMA system under fast Rician fading and partial-time partial-band jamming," *IEEE Trans. Commun.*, vol. 67, no. 10, pp. 7183–7194, Oct. 2019.
- [10] B. Smida, L. Hanzo, and S. Affes, "Exact BER performance of asynchronous MC-DS-CDMA over fading channels [transactions letters]," *IEEE Trans. Wireless Commun.*, vol. 9, no. 4, pp. 1249–1254, Apr. 2010.
- [11] L.-L. Yang and L. Hanzo, "Performance of generalized multicarrier DS-CDMA over Nakagami-m fading channels," *IEEE Trans. Commun.*, vol. 50, no. 6, pp. 956–966, Jun. 2002.
- [12] Y. Su, Y. Liu, Y. Zhou, J. Yuan, H. Cao, and J. Shi, "Broadband LEO satellite communications: Architectures and key technologies," *IEEE Wireless Commun.*, vol. 26, no. 2, pp. 55–61, Apr. 2019.
- [13] B. Akbil, B. Nsiri, G. Ferre, and D. Aboutajdine, "Carrier frequency offset estimation in MC-DS-CDMA systems with zero-IF receivers," in *Proc. IEEE ISVC. Conf.*, Dec. 2010, pp. 1–4.
- [14] L. Liu, X. Dai, and D. Li, "A novel pilot-based carrier frequency offset estimation in MC-DS-CDMA uplink," in *Proc. IET CCWSN*, Feb. 2009, pp. 1039–1042.
- [15] D. Lee, L. B. Milstein, and H. Lee, "Analysis of a multicarrier DS-CDMA code-acquisition system," *IEEE Trans. Commun.*, vol. 47, no. 8, pp. 1233–1244, Aug. 1999.
- [16] L.-L. Yang and L. Hanzo, "Performance of parallel code acquisition schemes for multicarrier CDMA over frequency-selective Rayleigh fading channels," in *Proc. IEEE PIMRC*, Aug. 2000, pp. 119–123.
- [17] L.-L. Yang and L. Hanzo, "Serial acquisition performance of single-carrier and multicarrier DS-CDMA over Nakagami-m fading channels," *IEEE Trans. Wireless Commun.*, vol. 1, no. 4, pp. 692–702, Oct. 2002.
- [18] S. Kondo and B. Milstein, "Performance of multicarrier DS CDMA systems," *IEEE Trans. Commun.*, vol. 44, no. 2, pp. 238–246, Feb. 1996.
- [19] U. Cheng, W. J. Hurd, and J. I. Statman, "Spread-spectrum code acquisition in the presence of Doppler shift and data modulation," *IEEE Trans. Commun.*, vol. 38, no. 2, pp. 241–250, Feb. 1990.
- [20] S. M. Kay, "Conclusion of important PDF," in *Fundamentals of Statistical Signal Processing*, 1st ed. Upper Saddle River, NJ, USA: Prentice-Hall, 1993, pp. 402–408.
- [21] R. Cochetti, "Low earth orbit (LEO) mobile satellite communications systems," in *Mobile Satellite Communications Handbook*, 1st ed. West Sussex, U.K.: Wiley, 2015, pp. 119–156.
- [22] G. L. Turin, "The characteristic function of Hermitian quadratic forms in complex normal variables," *Biometrika*, vol. 47, nos. 1–2, pp. 199–201, Jun. 1960.
- [23] R. R. Rick and L. B. Milstein, "Parallel acquisition in mobile DS-CDMA systems," *IEEE Trans. Commun.*, vol. 45, no. 11, pp. 1466–1476, Nov. 1997.



ENTONG MENG is currently pursuing the Ph.D. degree with the School of Information and Electronics, Beijing Institute of Technology. Her research interests include satellite communication, multi-carrier communication, and anti-interference technology.



XIANGYUAN BU (Member, IEEE) received the B.E. and Ph.D. degrees in communications engineering from the Beijing Institute of Technology (BIT), Beijing, China, in 1987 and 2007, respectively. He is currently a Professor with the School of Information and Electronics, BIT. His current research interests include satellite communications, channel coding theory, MIMO systems, and space time signal processing.